Quantum beats induced by spectral diffusion between independent two-level systems

C. Crépin*
Laboratoire de Photophysique Moléculaire, Bâtiment 210, Université Paris-Sud, 91405 Orsay Cedex, France
(Received 8 August 2002; published 6 January 2003)

We analyze theoretically the time-resolved signal detected in three-pulse, photon echo experiments where several independent two-level systems are involved, in a case when the time delay T between the two last pulses is much longer than delay τ between the two first pulses. A spectral diffusion process on a long time scale is included in the calculation of the τ-dependent response signal. If spectral diffusion occurs between the different systems, the signal exhibits quantum beats instead of the polarization interferences observed without spectral diffusion. This analysis provides different insights on dynamical processes and spectroscopy, as demonstrated in examples of experimental results obtained on vibrational dynamics of molecules embedded in matrices.

DOI: 10.1103/PhysRevA.67.013401 PACS number(s): 42.50.Md, 78.47.+p, 82.53.Kp

I. INTRODUCTION

Time-resolved four-wave mixing (TR FWM) experiments performed with short-pulse lasers are in constant development, especially for semiconductor nanostructures [1] and molecules in condensed phase [2]. These experiments give essential information on dynamical processes. We discuss in this paper one color TR FWM (OC TR FWM) experiments, usually named three-pulse photon echo experiments. Coherence, population relaxation, and also spectral diffusion processes can be studied from the observed signal related to the third-order polarization of the sample [3]. Ultrashort pulse sources allow the resonant excitation of different coupled or uncoupled transitions in the same spectral range. In specific cases, the resulting time-resolved signal involves oscillations corresponding to beat frequencies between pairs of these transitions. Analysis of these oscillations in terms of their period, phase, and amplitude provides information on their origins and on new properties of the samples [4–7].

Recently, we have carried out OC TR FWM experiments on vibrational transitions of small molecules (CO, DCl) embedded in van der Waals solids [8,9]. Different species can be excited in the same sample, e.g., monomers and dimers, isotopic $D^{35}Cl$ and $D^{37}Cl$, which have vibrational transitions with very close frequencies. We discuss here the total time integrated OC TR FWM signal versus time delay τ between the two first pulses in such kind of configurations that correspond to the coherent excitation of several species. Without spectral diffusion, the signal would exhibit polarization interferences [4] involving the response signals of each species. In the molecular systems we studied, spectral diffusion can occur on nanoseconds to microseconds time scales, a long time scale, due to intermolecular vibrational energy transfer between the trapped molecules (V-V transfers) [10]. The experimental setup, described in Ref. [8], is that of a two-pulse photon echo experiment, with only two directions of propagation of the laser beams; as the laser source (a free-electron laser) generates bunches of pulses, there are two bunches of pulses interacting with the sample. The third pulses (a bunch of third pulses) are thus the following ones in the bunch of either the first pulses or the second ones (cf. Fig. 1). The time delay T_r between the first and the third pulse, or between the second and the third pulse, is fixed : it is the inverse of the repetition rate of the pulses of the laser source. This delay is in the nanosecond range, much longer than the tunable time delay τ between the two first pulses in the tens of picoseconds. Spectral diffusion would be thus an important process to be taken into account during time T_r, and may be neglected during time delay τ.

In the first part of the paper, we evaluate theoretically the consequences of spectral diffusion on the detected signal and in the second part, we compare the model with the experimental results.

II. THEORETICAL CONSIDERATION

The signal results from the interaction of laser pulses following only two different wave vectors $\mathbf{k}_i$ and $\mathbf{k}_j$. It radiates in a fixed direction : $\mathbf{k}_s = 2\ \mathbf{k}_i - \mathbf{k}_j$. The notation used, from Mukamel's book [11], includes a time-ordered process : indices 1,2,3 for the first, second, and third pulse, respectively. There are two cases : (a) $\mathbf{k}_1 = \mathbf{k}_j$, followed by $\mathbf{k}_2 = \mathbf{k}_i$ and (b) $\mathbf{k}_1 = \mathbf{k}_i$, followed by $\mathbf{k}_2 = \mathbf{k}_j$, in any case $\mathbf{k}_3 = \mathbf{k}_i$. (a) and (b) correspond to positive and negative, respectively, delay τ in

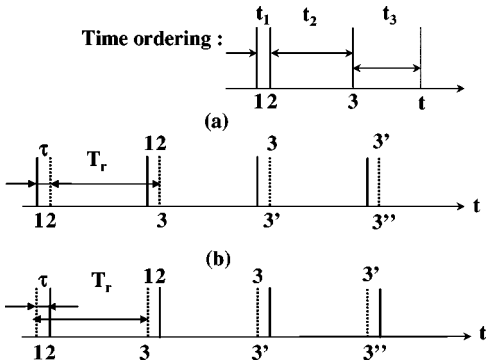

FIG. 1. Time ordering of the pulses: definition of times t_i on the top, of times τ and T_r in the experiments, (a) $\tau > 0$, (b) $\tau < 0$, pulses following wave vectors $\mathbf{k}_1$ and $\mathbf{k}_2$ in bold lines and dotted lines, respectively.

*Electronic address: claudine.crepin-gilbert@ppm.u-psud.fr

the stimulated photon echo signal (Fig. 1). For the remainder of the paper, we will use a notation in brackets [ ] for specific expressions corresponding to the (b) case. The wave vector of the fourth wave, the signal one, in (a) [(b)] case is $\mathbf{k}_s = \mathbf{k}_{a[b]} = \mathbf{k}_3 + [-]\mathbf{k}_2 - [+]\mathbf{k}_1$. The external field $\mathbf{E}(\mathbf{r},t)$ is

$$\begin{aligned} E(\mathbf{r},t) = & E_1(t+T+\tau')\exp[i(\mathbf{k}_1\mathbf{r}-2\pi\omega_l t)] \\ & + E_2(t+T)\exp[i(\mathbf{k}_2\mathbf{r}-2\pi\omega_l t)] + E_3(t) \\ & \times \exp[i(\mathbf{k}_3\mathbf{r}-2\pi\omega_l t)] + \text{c.c.}, \end{aligned}$$

where $\tau' > 0$ and $T > 0$ are the time intervals between pulses No. 1 and No. 2, and between pulses No. 2 and No. 3 respectively; (a) $\tau' = \tau$ and $T = T_r$, (b) $\tau' = -\tau$ and $T = T_r + \tau$. The time-integrated FWM detected signal $[S(\tau)]$ is related to component $\mathbf{k}_s = \mathbf{k}_3 \pm \mathbf{k}_2 \mp \mathbf{k}_1$ of the third-order nonlinear polarization $[P^{(3)}(t)]$ by $S(\tau) = \int_0^\infty dt |P^{(3)}(t)|^2$. Without spectral diffusion, $P^{(3)}(t)$ is given [11] by

$$\begin{aligned} P^{(3)}(t) = & \left(\frac{i}{\hbar}\right)^3 \int_0^\infty dt_3 \int_0^\infty dt_2 \int_0^\infty dt_1 \int_{-\infty}^{+\infty} d\omega g(\omega) \\ & \times R_{a[b]}(t_3,t_2,t_1,\omega)\exp\{2i\pi\omega_l(t_3-[+]t_1-t)\} \\ & \times E_3(t-t_3)E_2^{1[*]}(t+T-t_3-t_2) \\ & \times E_1^{*[1]}(t+T+\tau'-t_3-t_2-t_1). \end{aligned} \tag{1}$$

$t_{1,2,3}$ are the three ordered propagation periods till time t, between the action of pulses No. 1 and No. 2, No. 2 and No. 3, the action of pulse No. 3 and t, respectively (Fig. 1); $g(\omega)$ is the inhomogeneous distribution of transition frequencies; $R_{a[b]}(t_3,t_2,t_1,\omega)$ is the nonlinear-response function that contains all dynamical information [11–13].

We assume that the laser-pulse duration is short compared with molecular dynamical constants and $S(\tau)$ will be calculated in the impulsive limit $[E_i(t) = E_i\delta(t)]$.

A. Single two-level system

1. No spectral diffusion

For a single two-level system, invoking the rotating wave approximation, the nonlinear response function is written as

$$\begin{aligned} R_{a[b]}(t_3,t_2,t_1,\omega) = & N|\mu|^4\exp\{2i\pi\omega(t_1-[+]t_3)\} \\ & \times (\exp[-t_2/T_1]+\exp[-t_2/T_g]) \\ & \times \exp[-(t_1+t_3)/T_2], \end{aligned} \tag{2}$$

where μ is the transition dipole moment, N is the population of the two-level system according to the assumption that at $t=-\infty$, all the population is in the ground state, T_2 is the dephasing time of the transition, T_1 is the excited state relaxation time, and T_g is the ground-state recovery time.

Introducing $G(t)$, the Fourier transform of $g(\omega)$, and $\chi(t) = G(t)\exp(-2i\pi\langle\omega\rangle t)$, where $\langle\omega\rangle = \int_{-\infty}^{+\infty} d\omega\omega g(\omega)$ is the mean frequency of the transition, the inhomogeneous contribution is involved in a time function and we get

$$\begin{aligned} & \int_{-\infty}^{+\infty} d\omega R_{a[b]}(t_3,t_2,t_1,\omega)g(\omega) \\ & = G(t_1-[+]t_3)N|\mu|^4\exp[-(t_1+t_3)/T_2] \\ & \quad \times (\exp[-t_2/T_1]+\exp[-t_2/T_g]) \\ & = \chi(t_1-[+]t_3)R_{a[b]}(t_3,t_2,t_1,\langle\omega\rangle). \end{aligned} \tag{3}$$

In the general case of a symmetric inhomogeneous distribution $g(\omega)$ centered to $\langle\omega\rangle$, $\chi(t)$ is a real and even function.

Using Eq. (3), Eq. (1) becomes in the impulsive limit,

$$\begin{aligned} P^{(3)}(t) = & \left(\frac{i}{\hbar}\right)^3 \chi(\tau'-[+]t)R_{a[b]}(t,T,\tau',\langle\omega\rangle) \\ & \times E_3E_2^{1[*]}E_1^{*[1]}\exp(-[+]2i\pi\omega_l\tau'). \end{aligned} \tag{4}$$

Without any spectral diffusion, $S(\tau)$ is obtained from Eqs. (2) and (4),

$$S(\tau) = A\exp(-2|\tau|/T_2)\int_0^\infty dt|\chi(t-\tau)|^2\exp(-2t/T_2), \tag{5}$$

where $A = (1/\hbar)^6N^2|E_3E_2E_1|^2|\mu|^8[\exp(-T/T_1)+\exp(-T/T_g)]^2$. Equation (5) results in the well-known behavior of a homogeneous transition $[\chi(t)=1]$ with a symmetric decreasing of the signal versus $|\tau|$, and in that of a strongly inhomogeneous transition $[\chi(t)=\delta(t)]$ exhibiting a lifetime equal to $T_2/4$ for $\tau > 0$.

2. Total spectral diffusion

If spectral diffusion occurs during period T, the nonlinear-response function for a given transition frequency ω cannot be used in Eq. (1) and, in the case of characteristic diffusion times much shorter than delay T (total spectral diffusion), the integration over the last period (t_3) must be joined by another integration over the transition frequency distribution [3,8]. Equation (1) is recast in the form

$$\begin{aligned} P^{(3)}(t) = & \left(\frac{i}{\hbar}\right)^3 N|\mu|^4 \int_0^\infty dt_3 \int_0^\infty dt_2 \int_0^\infty dt_1 \int_{-\infty}^{+\infty} d\omega g(\omega) \\ & \times \exp[2i\pi\omega t_1]\int_{-\infty}^{+\infty} d\omega' g(\omega') \\ & \times \exp\{-[+]2i\pi\omega' t_3\}\exp\{2i\pi\omega_l(t_3-[+]t_1-t)\} \\ & \times \exp[-(t_1+t_3)/T_2](\exp[-t_2/T_1] \\ & + \exp[-t_2/T_g])E_3(t-t_3)E_2^{1[*]}(t+T-t_3-t_2) \\ & \times E_1^{*[1]}(t+T+\tau'-t_3-t_2-t_1). \end{aligned} \tag{6}$$

In the impulsive limit, we get

$$S(\tau) = A\exp[-2|\tau|/T_2]|\chi(\tau)|^2\int_0^\infty dt|\chi(t)|^2\exp[-2t/T_2]. \tag{7}$$

$S(\tau)$ is a symmetric function of τ, directly related to the Fourier transform of the absorption profile $\propto G(\tau)\exp[-|\tau|/T_2]$ [3].

B. *n*-two-level systems

$S(\tau)$ results from the summation of the nonlinear polarization over n systems: $P^{(3)}(t)=\Sigma_{i=1}^{n}P_i^{(3)}(t)$. The inhomogeneous distribution of frequencies is $g_{tot}(\omega)=\Sigma_{i=1}^{n}N_i g_i(\omega)/\Sigma_{i=1}^{n}N_i$ and, with $N=\Sigma_{i=1}^{n}N_i$, $G_{tot}(t)=\Sigma_{i=1}^{n}N_i\chi_i(t)\exp[2i\pi\langle\omega_i\rangle t]/N$, where N_i and $\langle\omega_i\rangle$ are the population and the mean frequency of system i, respectively, $\chi_i(t)$ is a real and even function, assuming that each system i has a symmetric inhomogeneous distribution of frequencies.

1. No spectral diffusion

Without any spectral diffusion, $P_i^{(3)}(t)$ is expressed by Eq. (4) and

$$P^{(3)}(t)=\left(\frac{i}{\hbar}\right)^3 E_3E_2^{1[*]}E_1^{*[1]}\exp\{-[+]2i\pi\omega_l\tau'\}\times\sum_{i=1}^{n}\{N_i|\mu_i|^4\chi_i(\tau'-[+]t)\exp\{2i\pi\langle\omega_i\rangle\times(\tau'-[+]t)\}\exp[-(t+\tau')/T_2^{(i)}](\exp[-T/T_1^{(i)}]+\exp[-T/T_g^{(i)}])\}. \quad (8)$$

In the experimental case analyzed in Sec. III, systems i correspond to vibrational transitions of different isotopic species or of different very weak complexes of the same molecule and we may assume

$$\forall i, T_2^{(i)}=T_2,\ \ T_1^{(i)}=T_1,\ \ T_g^{(i)}=T_g,\ \ \mu_i=\mu,$$

so that the total inhomogeneous distribution is directly included in Eq. (8) and

$$S(\tau)=A\exp[-2|\tau|/T_2]\int_0^\infty dt|G_{tot}(t-\tau)|^2\exp[-2t/T_2]. \quad (9)$$

In the case $n=2$, with the same inhomogeneous distribution for both transitions $[\chi_1(t)=\chi_2(t)=\chi(t)]$, using notations $\delta=\omega_2-\omega_1$ and $\alpha=N_2/N_1$, we have

$$S(\tau)=\frac{A}{(1+\alpha)^2}\exp[-2|\tau|/T_2]\int_0^\infty dt|\chi(t-\tau)|^2\times\exp[-2t/T_2]\{1+\alpha^2+2\alpha\cos[2\pi\delta(t-\tau)]\}. \quad (10)$$

Introducing $S_{0,c,s}$ functions as

$$S_0(\tau)=\int_0^\infty dt|\chi(t-\tau)|^2\exp[-2t/T_2],$$

$$S_c(\tau)=\int_0^\infty dt|\chi(t-\tau)|^2\exp[-2t/T_2]\cos[2\pi\delta t],$$

$$S_s(\tau)=\int_0^\infty dt|\chi(t-\tau)|^2\exp[-2t/T_2]\sin[2\pi\delta t], \quad (11)$$

we get

$$S(\tau)=\frac{A}{(1+\alpha)^2}\exp[-2|\tau|/T_2][(1+\alpha^2)S_0(\tau)+2\alpha\{\cos[2\pi\delta\tau]S_c(\tau)+\sin[2\pi\delta\tau]S_s(\tau)\}]. \quad (12)$$

This expression corresponds to the polarization interferences [4]. Homogeneous transitions result in

$$S(\tau)=\frac{A}{(1+\alpha)^2}\frac{T_2}{2}\exp[-2|\tau|/T_2]\left\{(1+\alpha^2)+\frac{2\alpha}{1+\pi^2\delta^2T_2^2}(\cos[2\pi\delta\tau]+\pi\delta T_2\sin[2\pi\delta\tau])\right\}.$$

The signal exhibits oscillations involving an asymmetry due to a dephasing time different from zero.

Large inhomogeneously broadened transitions result in $S(\tau)=A\exp[-4\tau/T_2]\theta(\tau)$, where $\theta(t)$ is the heaviside function : the signal has the same feature as that obtained with only one excited transition.

In Appendix A, the expression has been calculated using a Lorentzian shape for the inhomogeneous distribution. Examples of signals are represented in Figs. 2(a) and 2(b). The obtained analytic expression shows clearly that there is no modulation of the signal resulting from the rephasing process, i.e., the real photon echo process [cf. Fig. 2(a)].

2. Total spectral diffusion within the inhomogeneous distribution of each two-level system

We have to sum the expression Eq. (6) over indices i, where $g(\omega)$ and $g(\omega')$ represent the same inhomogeneous distribution. We get

$$P^{(3)}(t)=\left(\frac{i}{\hbar}\right)^3 E_3E_2^{1[*]}E_1^{*[1]}\exp\{-[+]2i\pi\omega_l\tau'\}\times\sum_{i=1}^{n}\{G_i(\tau')G_i(-[+]t)N_i|\mu_i|^4\times\exp[-(\tau'+t)/T_2^{(i)}](\exp[-T/T_1^{(i)}]+\exp[-T/T_g^{(i)}])\}, \quad (13)$$

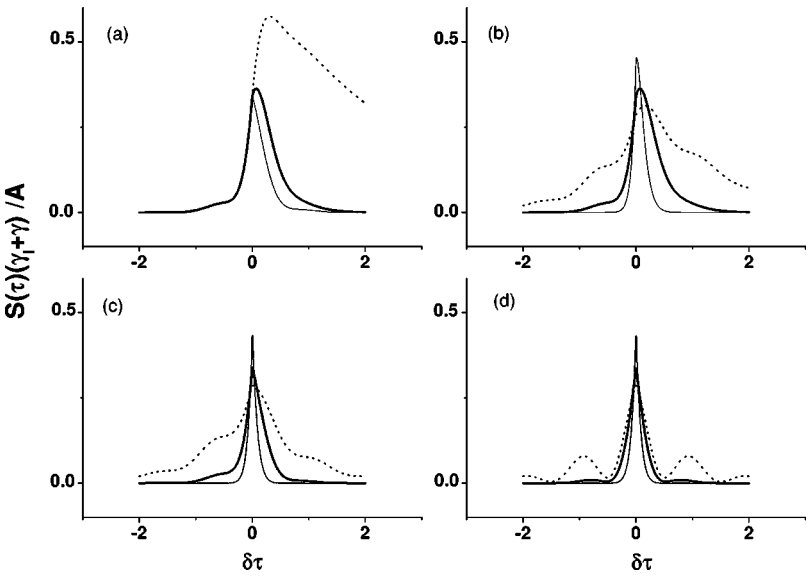

FIG. 2. Simulation of $S(\tau)$ on two two-level systems with an inhomogeneous Lorentzian distribution [(full width at half maximum) FWHM $=\gamma_l/\pi$]; $\gamma=1/T_2$, $\alpha=0.5$. (a) $\gamma+\gamma_l=2\delta$; $\gamma_l=19\gamma$ (dotted line), $\gamma_l=\gamma$ (bold line), $\gamma=19\gamma_l$ (gray line). (b), (c), and (d) $\gamma_l=\gamma$; $\gamma+\gamma_l=2\delta/3$ (dotted line), $\gamma+\gamma_l=2\delta$ (bold line), $\gamma+\gamma_l=6\delta$ (gray line). (a) and (b) Without spectral diffusion, Eqs. (12) and (A1); (c) total spectral diffusion within each system, Eqs. (14) and (A2); (d) total spectral diffusion within both systems, Eqs. (17) and (A3).

With n similar transitions in terms of T_2, T_1, T_g, μ, and $\chi(t)$, the expression of the signal is simplified

$$S(\tau)=A\exp[-2|\tau|/T_2]|\chi(\tau)|^2\int_0^\infty dt|\chi(t)|^2\exp[-2t/T_2]\times\left|\sum_{i=1}^{n}\frac{N_i}{N}\exp[2i\pi\langle\omega_i\rangle(t-\tau)]\right|^2.$$

Interferences between transition frequencies are expressed in the same way as in Eq. (9) by $|\Sigma_{i=1}^{n}(N_i/N)\exp[2i\pi\langle\omega_i\rangle(t-\tau)]|^2$. With $n=2$, using Eq. (11), $S(\tau)$ is given by

$$S(\tau)=\frac{A}{(1+\alpha)^2}\exp[-2|\tau|/T_2]|\chi(\tau)|^2[(1+\alpha^2)S_0(0)+2\alpha\{\cos[2\pi\delta\tau]S_c(0)+\sin[2\pi\delta\tau]S_s(0)\}]. \quad (14)$$

Within the envelope of $|\chi(\tau)|^2$, the asymmetry of the temporal signal, involving oscillations, appears with a behavior very similar to the case where no spectral diffusion occurs [cf. Eq. (12)]. This feature can be observed [Fig. 2(c)] with the expression developed in Appendix A.

3. Total spectral diffusion over the whole inhomogeneous distribution

In this case, the sum of the expression Eq. (6) over indices i must be performed with $g(\omega')$ covering all the inhomogeneous distributions $g_j(\omega')$, i.e., $g(\omega')$ becomes $\Sigma_{j=1}^{n}(N_j/N)g_j(\omega')$. We get

$$P^{(3)}(t)=\left(\frac{i}{\hbar}\right)^3 E_3E_2^{1[*]}E_1^{*[1]}\exp\{-[+]2i\pi\omega_l\tau'\}\times\sum_{i=1}^{n}\{N_iG_i(\tau')|\mu_i|^2\exp[-\tau'/T_2^{(i)}]\}\times\sum_{j=1}^{n}\left\{\frac{N_j}{N}G_j(-[+]t)|\mu_j|^2\times\exp[-t/T_2^{(j)}]\right\}f(T_{pop}), \quad (15)$$

where $f(T_{pop})$ is a function of T and of the different population times, very long compared to $T_2^{(i)}$; $f(T_{pop})=\exp[-T/T_1]+\exp[-T/T_g]$ in the case of n transitions involving similar population relaxation times. With n similar transitions in term of T_2, T_1, T_g, and μ, the expression of the signal is simplified

$$S(\tau)=A\exp[-2|\tau|/T_2]|G_{tot}(\tau)|^2\int_0^\infty dt|G_{tot}(t)|^2\times\exp[-2t/T_2]. \quad (16)$$

This expression is equivalent to Eq. (7) where we consider the set of n transitions as one inhomogeneous transition. $S(\tau)$ has thus a symmetric shape and is directly related to the Fourier transform of the whole absorption band $\propto G_{tot}(\tau)\exp[-|\tau|/T_2]$. If $n=2$ with $\chi_1(t)=\chi_2(t)=\chi(t)$,

$$S(\tau)=A\frac{|\chi(\tau)|^2}{(1+\alpha)^4}\exp[-2|\tau|/T_2](1+\alpha^2+2\alpha\cos[2\pi\delta\tau])\times\int_0^\infty dt|\chi(t)|^2\exp[-2t/T_2](1+\alpha^2+2\alpha\times\cos[2\pi\delta t]),$$

i.e.,

$$S(\tau)=A\frac{|\chi(\tau)|^2}{(1+\alpha)^4}\exp[-2|\tau|/T_2]\times(1+\alpha^2+2\alpha \times\cos[2\pi\delta\tau])[(1+\alpha^2)S_0(0)+2\alpha S_c(0)]. \quad (17)$$

There is no dephasing in the oscillations involved in $S(\tau)$ and the maximum of the signal is obtained at $\tau=0$, contrary to the results of Secs. II B 1 and II B 2 [Fig. 2(d)]. These modulations have the same behavior as modulations due to quantum beats obtained in OC TR FWM experiments in systems involving several transitions including a common level ($\vee$ or $\wedge$ diagrams) [4,14]. Spectral diffusion between the independent two-level systems induces an oscillating behavior in the nonlinear-response signal, similar to that of a system involving different transitions from the same energy level : spectral diffusion has mixed initially independent energy levels.

III. COMPARISON WITH EXPERIMENTS

The experimental results we discuss have been obtained on vibrational transitions of molecules isolated in matrices : DCl and CO in solid nitrogen. The bandwidths including homogeneous and inhomogeneous broadenings were measured from infrared absorption spectra of the samples. As DCl and CO are diatomic molecules with sizes very close to that of N_2, they are isolated in the well-defined subtitutional sites of the fcc structure of the nitrogen lattice. The inhomogeneous broadening results mainly from multipolar interactions between the guest molecules, and more precisely from dipolar interactions. Assuming a statistical distribution of the guest molecules in the lattice, these interactions produce a Lorentzian inhomogeneous distribution [10,15]. A detailed analysis of the CO/N_2 absorption profile reveals in fact a Voigt behavior [16]. We have used either Gaussian or Lorentzian $g(\omega)$ functions, corresponding to the limit cases, in order to calculate the time-resolved signal of CO/N_2 samples. Clear difference appears only for $\tau\approx 0$ and it does not affect the behavior of the modulation that we want to analyze. An example of both fits obtained with both of these inhomogeneous profiles is reported in Appendix B on an experimental result involving only 1 two-level system. For the following discussion, we choose to write function χ as $\chi(t)=\exp(-\gamma_l|t|)$, related to a Lorentzian inhomogeneous profile (FWHM$=\gamma_l/\pi$): it is in a good agreement with the experimental profiles and it gives simple analytic expressions (cf. Appendix A).

The reported experimental data exhibit a signal in the short time range of picoseconds or tens of picoseconds. Under these conditions, the relation $|\tau|\ll T_r$ (T_r is fixed to 16 or 32 ns), is always verified so that $T\approx T_r$ when $\tau<0$, and constant A defined in Sec. II A is the same whatever the sign of τ.

A. DCl in nitrogen matrices

DCl trapped in nitrogen matrices exhibits a complex absorption spectrum [17] because of the presence of DCl clusters. Even at low concentration, the spectroscopic feature of the DCl monomers involves four bands within ten wave numbers between 2062 and 2069 cm^{-1} : two for each isotopic species ($D^{35}Cl$ and $D^{37}Cl$) with one band assigned to the isolated molecule and another band assigned to the molecule close to another DCl molecule trapped in a next-nearest-neighbor site (nnn dimers). All these bands are coherently excited with the picosecond-laser source within its spectral width of 20 cm^{-1}. The experimental results obtained in the temperature range 7–25 K, involving samples with different concentrations are reported in Ref. [18]. We analyze here the signals obtained in the simplest case of a concentration of guest molecules, low enough to present only two absorption bands assigned to the isolated 35 and 37 isotopic species. The frequency shift involved is thus $\delta=3$ cm^{-1} $=0.09$ ps^{-1}. The vibrational transition characteristics are not significantly modified from an isotopic species to the other. The OC TR FWM signal can be described either by Eq. (12) if the *V-V* transfer rate is much smaller than $1/T_r$, or by Eq. (14) or (17) if the *V-V* transfer rate is much faster than $1/T_r$, with $\alpha=1/3$ from the natural isotopic abundances.

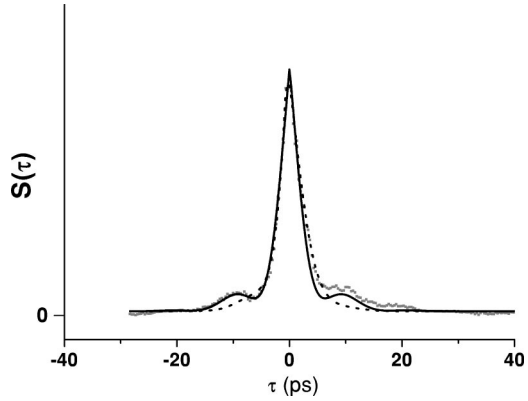

FIG. 3. Experimental data on a DCl/N_2 sample ($c=0.13\%$, $T=8$ K) (square points); curve fit using Eq. (A2) (dotted line); curve fit using Eq. (A3) (solid line), fits are obtained using $\alpha=1/3$ and $\delta=3$ cm^{-1} and lead to $\gamma_{tot}=0.16$ ps^{-1} and $\gamma_{tot}=0.10$ ps^{-1}, respectively; the second case gives a better agreement with experimental absorption data.

Experimental $S(\tau)$ exhibits clear oscillations at low temperature (7–10 K) (Fig. 3). There is a slight asymmetry between positive and negative times, with $S(\tau>0)\geqslant S(-\tau)$. Such a behavior occurs in the case of a real photon echo signal, where $S(\tau)$ provides from a rephasing of the different transition frequencies included in the inhomogeneous distribution. Nevertheless, the experimental signal cannot be fitted by Eq. (12) because when there is no spectral diffusion [cf. Eq. (A1)], the oscillations in the positive part $S(\tau>0)$ are smoothed compared with those in the negative part. If *V-V* transfers occur only between guest molecules of the same isotopic species, Eq. (A2) must be applied, but it cannot fit the experimental data. The signal derived from Eq. (A2), as from Eq. (A1), cannot reproduce the clear oscillation in the negative part. This clear oscillation is only reproduced with a very good agreement with the expression Eq. (A3) of the signal assuming *V-V* transfers between all the DCl molecules (Fig. 3). In fact, neglecting the small en-

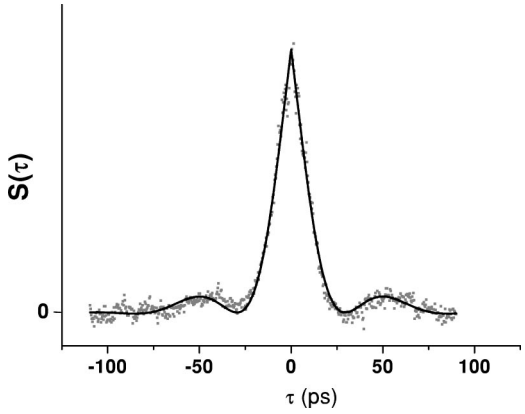

FIG. 4. Experimental data on a concentrated CO/N_2 sample ($c=1\%$), $T=20$ K (square points); curve fit using a modified expression of Eq. (A3) including two different inhomogeneous distributions (see text) leading to $\gamma_{tot}(CO)=0.033\ ps^{-1}=0.35\ cm^{-1}$ and $\gamma_{tot}[(CO)_2]=0.015\ ps^{-1}=0.16\ cm^{-1}$ (solid line).

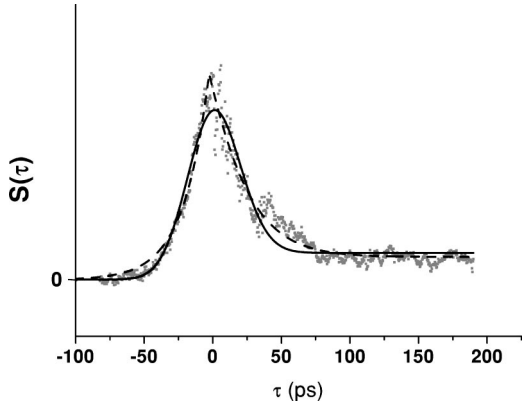

FIG. 5. Experimental data on a CO/N_2 sample ($c=0.2\%$, $T=11$ K) (square points); fits are obtained from expressions given in Ref. [8] including a partial spectral diffusion process characterized by the time constant T_d; curve fit using a Gaussian distribution (solid line): $T_d=26$ ns and $\gamma_{tot}=0.027\ ps^{-1}=0.48\ cm^{-1}$; curve fit using a Lorentzian distribution (dotted line): $T_d=23$ ns and $\gamma_{tot}=0.026\ ps^{-1}=0.27\ cm^{-1}$.

hancement of the signal in the positive part, the oscillations included in the experimental data are totally symmetric, which is the signature of spectral diffusion processes in the whole inhomogeneous distribution of the excited transitions. The slight enhancement observed for $\tau>0$ is, therefore, assigned to a weak rephasing process involving a small proportion of the molecules excited by the first pulse, as what was observed in experiments on CO/N_2 samples [8]. In the case of spectral diffusion, the coherence time cannot be determined from $S(\tau)$, only the total bandwidth $\gamma_{tot}=\gamma+\gamma_l$ is extracted from the fit of the experimental curve. The fit results in $\gamma_{tot}=0.10\pm0.01\ ps^{-1}$, whereas a value of $0.06\pm0.01\ ps^{-1}$ is deduced from the absorption spectrum of the sample. This discrepancy may be explained by the approximation included in Eq. (A3) neglecting the role of nnn dimers. Their coherent excitation induces oscillations with a periodicity twice as large as that the detected modulation : such oscillations cannot be clearly observed in the 20 ps range, but they shorten the signal, leading to a broadening of γ_{tot} deduced from the time-resolved experiments.

B. Concentrated samples of CO/N_2

Time-resolved experiments on the CO vibration in solid nitrogen have demonstrated that *V-V* transfers among the isolated CO molecules are very efficient for a concentration $c>0.2\%$, involving characteristic times less than 15 ns at $T>20$ K [8]. For $T>20$ K, $S(\tau)$ is assumed to result from total spectral diffusion processes taking into account experimental delay $T_r=32$ ns. In the case of concentrated samples ($c=1\%$), weak and symmetric oscillations are observed (Fig. 4) : $S(\tau)$ reproduces the expected features described in Sec. II B 3, involving two independent two-level systems. The analysis of the modulation reveals a beat frequency corresponding to $\delta=0.583\pm0.005\ cm^{-1}$. Absorption spectra of these samples have been recorded using a low resolution ($0.35\ cm^{-1}$) and only one vibrational band, assigned to CO stretching mode, has been detected. This band exhibits a slight asymmetry with a blue wing larger than the red one. We deduced that two bands were hidden in this absorption spectrum, the weakest band involving a blue shift of $+0.58\ cm^{-1}$ from the main one. As the oscillations appear only for a high concentration, the weak band is assigned to CO dimers isolated in solid N_2. This assignment is in agreement with previous works in matrices on CO absorption spectra : the stretching mode of $(CO)_2$ is observed with a blue shift in Ar and Kr matrices (shifts are $+1.4$ and $+1.2\ cm^{-1}$, respectively) [19], whereas calculations have evaluated it to $+0.3\ cm^{-1}$ [20]. The fit of the experimental time-resolved signal using Eq. (A3) overestimates α to 2/3 in disagreement with the ratio $[(CO)_2]/[CO]=0.13$ evaluated from a statistical distribution of CO molecules in the lattice for $c=1\%$. A smaller value $\alpha=0.37$ is deduced from the fit shown in Fig. 4 obtained from Eq. (16) assuming two different inhomogeneous Lorentzian distributions for the two transitions. We have, thus, verified that the parameters deduced from the fit agree with the low resolution absorption spectrum of the sample, indicating that $[(CO)_2]/[CO]=0.13$ may be underestimated. In this example, the time-resolved experiments have revealed the transition frequency of the CO dimer in solid nitrogen and the efficiency of *V-V* transfers between monomers and dimers.

IV. CONCLUSION

The OC TR DFWM signals give a clear signature of spectral diffusion processes. We have demonstrated that, under the coherent excitation of several independent two-level systems, they reveal whether or not spectral diffusion connects the different systems. In the experimental examples described, spectral diffusion occurs from energy transfers between isolated species in a solid sample. It is well known that such energy transfer can occur between different species.

The time-resolved experiments show, therefore, whether or not these energy transfers are more efficient between the same species than between all the species that can be coherently excited. Other spectral diffusion processes may be examined in the same way, for example, spectral diffusion due to the formation or the dissociation of molecular complexes embedded in a solid or a liquid. If different complexes involving the same chromophor molecule have close transition frequencies, the described time-resolved signals may be detected. The total spectral diffusion process may reveal the existence of the different complexes, not detected in absorption spectra because of the nonresolved large inhomogeneous bands.

ACKNOWLEDGMENTS

I wish to gratefully acknowledge the authors of the experimental results described here: Professor H. Dubost, Professor P. Roubin, A. Cuisset, Dr. J. M. Ortéga, and the technical assistance of CLIO; and especially Dr. M. Broquier and Dr. J. P. Galaup for helpful advice and discussions.

APPENDIX A: $S(\tau)$ WITH A LORENTZIAN INHOMOGENEOUS DISTRIBUTION

The analytic expressions of $S(\tau)$ are obtained using $\chi(t)=\exp(-\gamma_l|t|)$ and the notation $\gamma=1/T_2$. Equation (12) becomes

$$S(\tau)=\frac{A}{(1+\alpha)^2}\left(\theta(\tau)\left\{\exp[-4\gamma\tau]\left[(1+\alpha^2)\frac{\gamma_l}{\gamma_l^2-\gamma^2}+\alpha\left(\frac{1}{\gamma_l+\gamma}\frac{1}{1+\dfrac{\pi^2\delta^2}{(\gamma_l+\gamma)^2}}+\frac{1}{\gamma_l-\gamma}\frac{1}{1+\dfrac{\pi^2\delta^2}{(\gamma_l-\gamma)^2}}\right)\right]\right.\right.$$
$$\left.\left.-\frac{\exp[-2(\gamma_l+\gamma)\tau]}{2(\gamma_l-\gamma)}\left[1+\alpha^2+\frac{2\alpha}{1+\dfrac{\pi^2\delta^2}{(\gamma_l-\gamma)^2}}\left(\cos[2\pi\delta\tau]+\frac{\pi\delta}{\gamma-\gamma_l}\sin[2\pi\delta\tau]\right)\right]\right\}+\frac{\theta(-\tau)}{2(\gamma_l+\gamma)}\exp[-2(\gamma_l+\gamma)|\tau|]$$
$$\times\left[1+\alpha^2+\frac{2\alpha}{1+\dfrac{\pi^2\delta^2}{(\gamma_l+\gamma)^2}}\left(\cos[2\pi\delta\tau]+\frac{\pi\delta}{\gamma_l+\gamma}\sin[2\pi\delta\tau]\right)\right]\Bigg). \tag{A1}$$

Equation (14) becomes

$$S(\tau)=\frac{A}{2(\gamma+\gamma_l)(1+\alpha)^2}\exp[-2(\gamma+\gamma_l)|\tau|]\left[1+\alpha^2+\frac{2\alpha}{1+\dfrac{\pi^2\delta^2}{(\gamma+\gamma_l)^2}}\left(\cos[2\pi\delta\tau]+\frac{\pi\delta}{\gamma+\gamma_l}\sin[2\pi\delta\tau]\right)\right]. \tag{A2}$$

Equation (17) becomes

$$S(\tau)=\frac{A}{2(\gamma+\gamma_l)(1+\alpha)^4}\exp[-2(\gamma+\gamma_l)|\tau|](1+\alpha^2+2\alpha\cos[2\pi\delta\tau])\left(1+\alpha^2+\frac{2\alpha}{1+\dfrac{\pi^2\delta^2}{(\gamma+\gamma_l)^2}}\right). \tag{A3}$$

APPENDIX B: COMPARISON BETWEEN A LORENTZIAN AND A GAUSSIAN INHOMOGENEOUS DISTRIBUTION

We have simulated the experimental data obtained for CO/N_2 (1/200) samples where only one vibrational transition (CO stretching mode) was excited. In the case of a partial spectral diffusion during the interaction with the three laser pulses, the behavior of $S(\tau\sim 0)$ has been carefully investigated because it depends on the characteristic diffusion time (T_d) [8]. As the experimental absorption spectrum has been successfully fitted using a Voigt profile, a Lorentzian and a Gaussian inhomogeneous distributions are limit cases. We use, therefore, both analytic expressions of the inhomogeneous distributions in order to reproduce the time-resolved data: the Lorentzian limit [$\chi_l(t)=\exp(-\gamma_l|t|)$] and the Gaussian limit [$\chi_g(t)=\exp(-\gamma_g^2t^2)$]. Both best curve fits are reported in Fig. 5. Differences are not very important and, in particular, both fits lead to the same main characteristic diffusion time T_d.

[1] P. Borri, W. Langbein, S. Schneider, U. Woggon, R.L. Sellin, D. Ouyang, and D. Bimberg, Phys. Rev. Lett. **87**, 157401 (2001); S. Nishikawa, S. Kohmoto, H. Nakamura, Y. Sugimoto, N. Ikeda, T. Ishikawa, T. Akiyama, H. Ishikawa, and O. Wada, Physica E (Amsterdam) **13**, 273 (2002); D.M. Mittleman, R.W. Schoenlein, J.J. Shiang, V.L. Colvin, A.P. Alivisatos, and C.V. Shank, Phys. Rev. B **49**, 14 435 (1994), and references therein.

[2] J. Stenger, D. Madsen, J. Dreyer, P. Hamm, E.T.J. Nibbering, and T. Elsaesser, Chem. Phys. Lett. **354**, 256 (2002); M. Lim and R.M. Hochstrasser, J. Chem. Phys. **115**, 7629 (2001); W.P. de-Boeij, M.S. Pshenichnikov, and D.A. Wiersma, Chem. Phys. **233**, 287 (1998), and references therein.

[3] A.M. Weiner, S. De Silvestri, and E.P. Ippen, J. Opt. Soc. Am. B **2**, 654 (1985).

[4] J. Erland and I. Balslev, Phys. Rev. A **48**, R1765 (1993), and references therein.

[5] A. Tokmakoff, A.S. Kwok, R.S. Urdahl, R.S. Francis, and M.D. Fayer, Chem. Phys. Lett. **234**, 289 (1995).

[6] P. Hamm, M. Lim, M. Asplund, and R.M. Hochstrasser, Chem. Phys. Lett. **301**, 167 (1999).

[7] Jon-Paul R. Wells, C.W. Rella, I.V. Bradley, I. Galbraith, and C.R. Pidgeon, Phys. Rev. Lett. **84**, 4998 (2000).

[8] C. Crépin, M. Broquier, H. Dubost, J.P. Galaup, J.L. Le Gouët, and J.M. Ortéga, Phys. Rev. Lett. **85**, 964 (2000).

[9] M. Broquier, A. Cuisset, C. Crépin, H. Dubost, and J.P. Galaup, J. Lumin. **94-95**, 575 (2001).

[10] M. Harig, R. Charneau, and H. Dubost, Phys. Rev. Lett. **49**, 715 (1982).

[11] S. Mukamel, *Principles of Nonlinear Optical Spectroscopy* (Oxford University Press, New York, 1995).

[12] S. Mukamel and R.F. Loring, J. Opt. Soc. Am. B **3**, 595 (1986).

[13] Y.J. Yan and S. Mukamel, J. Chem. Phys. **94**, 179 (1991).

[14] M. Koch, J. Feldmann, G. von Plessen, E.O. Göbel, P. Thomas, and K. Köhler, Phys. Rev. Lett. **69**, 3631 (1992).

[15] A.M. Stoneham, Rev. Mod. Phys. **41**, 82 (1969).

[16] M. Harig, R. Charneau, and H. Dubost, J. Lumin. **24**, 643 (1981).

[17] D. Maillard, A. Schriver, J.P. Perchard, and C. Girardet, J. Chem. Phys. **71**, 505 (1979).

[18] M. Broquier, C. Crépin, A. Cuisset, H. Dubost, J. P. Galaup, and P. Roubin (unpublished).

[19] H. Dubost, Chem. Phys. **12**, 139 (1976).

[20] H. Dubost and L. Abouaf-Marguin, Chem. Phys. Lett. **17**, 269 (1972).